2012 IEEE International Conference on Robotics and Automation
RiverCentre, Saint Paul, Minnesota, USA
May 14-18, 2012

A Model and Formal Analysis of Braitenberg Vehicles 2 and 3

Iñaki Rañó

Abstract— **Braitenberg vehicles have attracted many students to work in robotics because of their apparent simplicity as control mechanisms. However, the lack of a formal theory supporting them entails they are used by the robotic community only as a teaching tool. This paper presents the first joint theoretical and comprehensive analysis of the behaviour of Braitenberg vehicles 2 and 3. The presented mathematical model of the vehicles is a non-linear dynamical system which is analysed for general conditions. This work paves the way to a proper and complete understanding of Braitenberg vehicles through a new theoretical framework. This framework allows the exploration of new applications and shows the need of stimulus analysis to drive its behaviour.**

I. Introduction

Braitenberg vehicles [1] qualitatively model sensor based animal steering and have long been used used on an empirical basis in robotics, but also in other fields like Artificial Life [2] [3]. In general, imitation of the natural world has provided very interesting results in Artificial Intelligence like, Genetic Algorithms, Artificial Neural Networks, Swarm Optimisation and so on. In the case of the simplest Braitenberg vehicles, what is modelled is the motion of animals towards, or escaping from, a stimulus, known in biology as positive or negative taxis behaviour [4]. Animals are very good at moving in the real world and, therefore, a good model to follow when implementing robotic motion. While positive taxis is a goal seeking technique, negative taxis implements avoidance behaviours, very common tasks needed by mobile robots. Moreover, as these models work at the steering or guidance level they can be used with any locomotive configuration. On the other hand, because of their simplicity, they are easily understood without the need of a strong formal background. In fact, as a control mechanism for wheeled robots, they are easier to understand by the newcomer to robotics than potential field approach based techniques. That is the reason why they are so often used to teach [5] [6].

Different Braitenberg vehicles have been used to provide robots with several abilities on an experimental basis. The work in [7] implements target acquisition using vehicle 3a, to perform phototaxis, in a combination with a modified version of vehicle 2b, to avoid obstacles through infrared sensors. Inspired by this work, [8] presents a wandering mechanism based on a combination of vehicle 2b with an artificial stimulus built up from laser and sonar proximity readings. The stimulus to implement vehicle 2b is just a weighted integration of the free area in front of the robot. Using fuzzy controllers that generate offset velocities on each wheel, Braitenberg vehicles 3a and 2b are used for local navigation in [9]. Goal seeking is implemented by vehicle 2b while vehicles 3b and 2a are used to avoid obstacles in the front and back of the robot respectively. A Lego vehicle with a hardware implementation of the vehicle 3b for obstacle avoidance and a wall following behaviour is presented in [10]. The power supply of the wheels is connected in a decreasing way to infrared sensors placed in the front of the robot, which makes the vehicle to slow down when objects are detected. An experimental analysis of vehicles 3a and 3b for odour source localisation is presented in [11], where the connection between sensors and motors is linear but sensor readings are normalised and averaged. Due to the nature of the stimulus and sensing hardware, there is a necessary sensor preprocessing that introduces a dynamic component on the connection, and, as we will see, it is not a 3 type Braitenberg vehicle in a strict sense. A four neuron model of cricket phonotaxis built with spiking units, comparable to the combination of vehicles 2a and 3b, is presented in [12]. A neural network, following the inspiration of Braitenberg vehicles 2a and 2b, was also used to implement several reflex responses of arthropods to optical flow patterns [13]. Inspired by Braitenberg's work, [14] presents a foraging robot neural controller with neuromodulation, a change on the behaviour of neurons allowing a switch between vehicle types 2b and 3b.

Through the literature we find multiple empirical applications of Braitenberg vehicles, ranging from target seeking, wandering, sound source localisation to obstacle avoidance. Besides these empirical applications, some theoretical results about Braitenberg vehicles have been already obtained. Some stability conditions for vehicle 3a are presented in [15]. It has been also proved that vehicle 2b, under some circumstances densely covers some parts of its workspace [16] while some times it also behaves as a billiard ball bouncing in a pool table [17], even when there are obstacles inside. This paper contributes to the general knowledge of Braitenberg vehicles as it provides a join mathematical model of the control mechanisms of vehicles 2 and 3. We analyse the dynamical system describing them and show new theoretical results of their behaviour. It is worth noting that all the results are analytical and therefore they do not require any experimental validation, however, simulations are presented to illustrate the theoretical results.

The rest of the paper is organised as follows. Section II reviews qualitative models of Braitenberg vehicle 2 and 3, states the working assumptions and presents the corresponding mathematical models of the controllers. The results of analysing the controllers is used to justify the qualitative understanding which was the basis of all previous empirical

Iñaki Rañó is with the Institute für Neuroinformatik, Ruhr-Universität-Bochum, Germany. inaki.rano@ini.rub.de

works. Section III derives general properties of the behaviour of the vehicles. As the assumptions on this section are also general and the model of the vehicles is a set of non-linear differential equations, the results are general and very helpful for design purposes. The simulations to illustrate the properties of the vehicle trajectories are presented in Section IV. A summary of the results, their implications and further working lines are presented in Section V.

II. Assumptions and Models of Vehicles 2 and 3.

By building up vehicles with sensors wired to their wheels, Braitenberg models complex behaviours with great simplicity. Wheels abstract locomotion to focus on steering, therefore, they model walking, swimming or crawling. This simplifies the control and analysis of motion, and is a good approximation as forward moving animals suffer from non-holonomic restrictions to motion [18]. Therefore Braitenberg vehicles can be used to design robotic controllers at the steering level. The sensors used by Braitenberg perceive an abstract stimulus at some point of the space, though it does not need to be a real stimulus, as it can be artificially constructed. To simulate the omni-directionality of the sensors many empirical applications of Braitenberg vehicles include rings of sensors. The vehicles considered here simply consist on direct or crossed connections between the sensors and the motors. Some vehicles have increasing connections such that the stronger the stimulus in the sensor gets the faster the associated wheels turn, while others have a decreasing connection. Figure 1 shows the various configurations these vehicles can display, though what increasing or decreasing connection means is not formally defined in [1].

A. A Quick Review of the Qualitative Behaviour

The vehicles, as animals, are immersed in environments with non negative bounded stimuli they can perceive through their sensors. For vehicles 2 and 3 a single stimulus is present in their environment, which, on the one hand, simplifies the analysis and, on the other hand, serves as building block for more complex vehicles. The combination of direct, crossed, increasing and decreasing connections between the sensors and the wheels of the vehicles generates four different vehicles as presented in Figure 1. When sensors on one side are connected to the motors on the same side we will talk about a-type vehicles, while b-type vehicles shown a crossed connection as depicted in figures 1(b) and 1(d). Vehicles 2 have an increasing connection linking perception to action, represented by the '+' sign on figures 1(a) and 1(b), while for vehicles 3 the connection is decreasing.

The behaviour of each vehicle can be analysed qualitatively by assuming a stimulus source, generating a distance decreasing scalar field, is located next to it. Basically, intuition indicates that vehicles 2b and 3a will move towards high values of stimuli, while vehicles 2a and 3b will head towards lower values. While vehicles 2 might move faster next to the stimulus source, vehicles 3 will slow down when they get close to high stimulus intensity because of the decreasing connection. All these vehicles intuitively generate gradient descent or hill climbing trajectories, while accounting for the additional non-holonomic constrains to their trajectories. The simplicity of the control mechanism makes it biologically plausible, while at the same time produces quite complex behaviours depending on the specific stimulus.

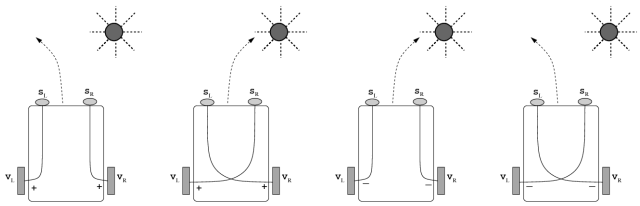

(a) Vehicle 2a (b) Vehicle 2b (c) Vehicle 3a (d) Vehicle 3b

Fig. 1. Schematics of Braitenberg Vehicles 2 and 3

Just as in the original work of Braitenberg we will assume the environment consists on a single stimulus the vehicle can measure without any disturbing noise, and therefore it can be modelled as a smooth function, a two dimensional non-negative C^2 function $S(\mathbf{x})$ of the position $\mathbf{x} \in D \subset \Re^2$, where D is a simply connected subset of $\Re^2$. The direct relation between the perceived stimulus and the velocity of the wheels can be modelled as a C^2 function $F(s)$ taking non negative values. This function is increasing for vehicles version 2 and decreasing for vehicles 3, which actually implies it has positive or negative derivative respectively on its domain, i.e. $F'(s) > 0$ for vehicle 2 and $F'(s) < 0$ for vehicle 3. Therefore, we can write $v_{R/L} = F(s)$ where 's' is the stimulus value on the sensor and '$v_{R/L}$' is the speed of the wheel. The restriction on the image of $F(s)$ being $\Re^+ \cup \{0\}$ forbids the vehicle to move backward, a biologically plausible assumption as animals do not walk backwards.

B. Controller of Braitenberg Vehicles

Given the above assumptions we can now derive a mathematical expression for the controller and compare its analysis with what intuition says about Braitenberg vehicles. Figure 2 shows the configuration of the sensors in the front of the vehicle. We will denote $\mathbf{x}$ the midpoint and δ the distance between the sensors. Since the vehicle has a heading direction θ, we can define a reference frame linked to the front of the vehicle $\hat{e}^T = [\cos\theta, \sin\theta]$ pointing in the direction of the vehicle motion and $\hat{e}_p^T = [-\sin\theta, \cos\theta]$, a unit vector orthogonal to $\hat{e}$, pointing to the left side of the vehicle. Approximating the function composition $F(S(\mathbf{x}))$ as a Taylor series around the mid point between the sensors and transforming wheel velocities into global velocities, we obtain:

$$v \approx F(S(\mathbf{x})) + \frac{\delta^2}{4}\hat{e}_p^T D^2 F(S(\mathbf{x}))\hat{e}_p \quad (1)$$

$$\omega \approx \mp\frac{\delta}{d}\nabla F(S(\mathbf{x}))\hat{e}_p \quad (2)$$

where d is the wheelbase, $\nabla F(S(\mathbf{x})) = \frac{dF}{dS}\nabla S(\mathbf{x})$ is the gradient of the composite function, $D^2F(S(\mathbf{x})) =$

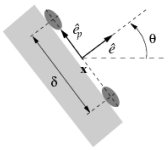

Fig. 2. Coordinate system at the Front of the vehicle

$\frac{d^2F}{dS^2}\nabla S(\mathbf{x})\nabla^T S(\mathbf{x}) + \frac{dF}{dS}D^2S(\mathbf{x})$ is the Hessian matrix, and the different signs on equation (2) correspond a-type (minus) and b-type (plus) vehicles. These equations are the result of a second order Taylor approximation of the wheel velocities.

Equation (1) shows that the first order approximation of the linear velocity of the vehicle depends on the value of the function $F(s)$ evaluated at the mid point between the sensors. This matches our intuition on how the vehicle with two sensors will behave as higher values of the stimulus $S(\mathbf{x})$ generate higher linear velocities for vehicles 2 and lower ones for vehicles 3. It is worth noting the velocity equation is independent on the type of vehicle 'a' or 'b', but the properties of $F(s)$ are very different for each vehicle. The error on the approximation depends on second order terms, i.e. on the Hessian of $F(S(\mathbf{x}))$, evaluated at the midpoint between the sensors. Therefore, the real vehicle can be faster or slower than the approximated one depending on the curvatures of the stimulus at the linearisation point. However, for a planar stimulus the approximation of the linear velocity will be exact.

The approximation for the angular velocity ω shows that the turning rate depends on the directional derivative of the stimulus along the direction of the sensors, orthogonal to the vehicle heading. Equation (2) can be written as $\omega = \mp\frac{\delta}{d}\partial_{\hat{e}_p}F(S(\mathbf{x}))$, where $\partial_{\hat{e}_p}$ represents the directional derivative along the direction of $\hat{e}_p$ and this velocity is multiplied by the morphological scaling factor $\frac{\delta}{d}$. This is the result of sampling the stimulus at two different points. Assuming, to simplify the analysis, the vehicle forward speed is zero, the gradient at one point $\mathbf{x}_0$ will be a constant vector we can write as $F'(S(\mathbf{x}_0))||\nabla S(\mathbf{x}_0)||\hat{e}_{\theta_0}$, where the sign of $F'(S(\mathbf{x}_0))$ is different for vehicles 2 and 3, $||\nabla S(\mathbf{x}_0)||$ is the module of the gradient at $\mathbf{x}_0$ and $\hat{e}_{\theta_0} = [\cos\theta_0, \sin\theta_0]^T$ is a unit vector along the direction of the gradient. Since $\omega = \dot{\theta}$, we can rewrite the angular velocity equation for a vehicle standing at a point as:

$$\dot{\theta} \;=\; \mp\frac{\delta}{d}F'(S(\mathbf{x}_0))||\nabla S(\mathbf{x}_0)||\sin(\theta_0 - \theta) \qquad (3)$$

The dynamical system (3) has two equilibrium points, specifically $\theta = \theta_0$ and $\theta = \theta_0 + \pi$, which correspond to the gradient and opposite directions. One equilibrium point will be stable and one unstable, though to identify the stable one we need to consider the sign of $F'(s)$. It can be seen that vehicles with $F'(s) > 0$ and minus sign (vehicle 2a) or $F'(s) < 0$ and plus sign (vehicle 3b) on equation (2) align their heading with the gradient as the stable equilibrium point is θ_0. The other vehicles perform a gradient descent on the stimulus. It is worth noting that the slope of $F(s)$ has a direct impact on the relaxation time of the angular controller, and therefore to make the vehicle turn faster for a given stimulus we need a steeper $F(s)$ function.

The performed analysis is also valid for any C^1 stimulus and $F(s)$ function regardless of whether they are positive or whether $S(\mathbf{x})$ has any extrema at all. Clearly, the smaller the distance between the sensors the more accurate the approach will be. Even though the analysis performed so far formally explains our intuition on how Braitenberg vehicles work, it is not enough, as the controlled variables are linked and, therefore, a deeper analysis is needed.

III. General Analysis of the vehicles behaviour

To analyse the general trajectories of the vehicles we will substitute the first term approximation of the velocities, equations (1) and (2), in the unicycle motion model to obtain:

$$\dot{x} \;=\; F(S(\mathbf{x}))\cos\theta \qquad (4)$$

$$\dot{y} \;=\; F(S(\mathbf{x}))\sin\theta \qquad (5)$$

$$\dot{\theta} \;=\; \mp\frac{\delta}{d}\nabla F(S(\mathbf{x}))\cdot\hat{e}_p \qquad (6)$$

where $\mathbf{x} = [x, y]^T$. Even though these equations model simultaneously vehicles 2 and 3 the actual shape of $F(S(\mathbf{x}))$ is very different for each vehicle, and we have to analyse each case separately. The general analysis of such a non linear dynamical system can be very complex even when equilibrium points or limit cycles can be found which is not usually the case.

To begin with the analysis we will assume the value of the stimulus falls between two values s_0 and s_1, i.e. $s_0 \leq S(\mathbf{x}) \leq s_1$ for all $\mathbf{x} \in D$, such that $S(\mathbf{x}) = s_0 \iff \mathbf{x} \in \partial D$, the lowest value appears at the workspace boundary. So far we assumed $F(s)$ is non-negative but we will impose the additional constraint of $F(s_0) = 0$ for vehicles 2, and $F(s_1) = 0$ for vehicles 3, while the function value at the other end is bounded. These conditions are imposed to obtain equilibrium points in the corresponding dynamical system as this is the only way of having the two equations (4) and (5) become zero simultaneously. In fact, these conditions should be imposed to empirical applications of Braitenberg vehicles.

A common technique to analyse the stability of an equilibrium point is the linear stability test, i.e. to analyse the eigenvalues of the Jacobian matrix. In our case the Jacobian matrix can be stated as:

$$J \;=\; \begin{bmatrix} \nabla F(S(\mathbf{x}))\hat{e}^T & F(S(\mathbf{x}))\hat{e}_p \\ \mp\frac{\delta}{d}\nabla F_{x|y}(S(\mathbf{x}))^T\hat{e}_p & \pm\frac{\delta}{d}\partial_{\hat{e}}F(S(\mathbf{x})) \end{bmatrix} \qquad (7)$$

where $\nabla F_{x|y}(S(\mathbf{x}))^T\hat{e}_p$ is a row sub-matrix containing the partial derivatives of the gradient w.r.t. x and y, and $\partial_{\hat{e}}F(S(\mathbf{x}))$ is the directional derivative of $F(S(\mathbf{x}))$ along $\hat{e} = [\cos\theta, \sin\theta]^T$. This matrix can be evaluated at the equilibrium points and the corresponding controller will have a stable equilibrium point if all the eigenvalues are negative and an unstable one otherwise.

A. Vehicles 2

Under the assumption that the stimulus takes its minimum value on the boundary ∂D, it can be proved that the trajectories of the vehicles 2 are actually bounded by ∂D, and therefore their motion is restricted to D. As the trajectories are the integral lines of the flow defined by the dynamical system given by equations (4), (5) and (6), to test whether the vehicle crosses an orientable surface we need to check if the flow has any non tangent component to the surface. In the case at hand, as the state space of the vehicle is (x, y, θ), the surface will be defined by the Cartesian product $\partial D \times S^1$. The first two components of the vector field defined by the dynamical system vanish at the boundary, while the third one will only vanish for angles θ orthogonal to the surface. If we define the normal vectors to the surface $\partial D \times S^1$, we can see they have no angular component and therefore the dot product of the surface normal and the flow defining the vehicle motion is zero, either because they are orthogonal to each other or because the flow completely vanishes. This effectively means no flow comes out of the surface and, therefore, vehicle 2 motion will be bounded by the contour ∂D in the workspace. We can restrict the motion of a Braitenberg vehicle on a stimulus field $S(\mathbf{x})$ by selecting a level curve with a value s_0 and a controller function $F(s)$ such that $F(s_0) = 0$. This design criterion is derived from the presented theoretical model and has not been explicitly identify before.

Since $F(S(\mathbf{x})) \neq 0$ in the interior of D the equilibrium points of both vehicle types, a and b, lay in the workspace boundary ∂D, the only points where equations (4) and (5) vanish simultaneously. Moreover, the equilibrium points can be obtained by solving $\nabla S(\mathbf{x})^T \hat{e}_p = 0$ for any $\mathbf{x} \in \partial D$, which gives at least two solutions for θ, as for each point $\mathbf{x} \in \partial D$ we can find two complementary angular values which make $\dot{\theta} = 0$. If the gradient of $S(\mathbf{x})$ vanishes at some points of ∂D, these points will belong to the equilibrium set. If the functions $F(s)$ and $S(\mathbf{x})$ are C^2, the gradient will be continuous along the boundary and, therefore, two closed curves formed by equilibrium points exist on the surface $\partial D \times S^1$ for vehicles 2.

We know equilibrium points exist for these systems and we can use the Jacobian matrix to perform a linear stability test of all those points. In the case of the gradient vanishing in ∂D, if we substitute $F(S(\mathbf{x})) = 0$ and $\nabla S(\mathbf{x}) = \mathbf{0}$ in (7) we obtain only zero eigenvalues and therefore this test gives no information about the stability of the equilibrium set $\partial D \times S^1$. We need to apply more sophisticated methods as presented for the two dimensional case in [19]. However, if the gradient of the stimulus is not zero at the boundary, the eigenvalues of the Jacobian matrix can be computed and they indicate the stability of the equilibrium points. While one of them will always be zero, for the vehicle 2a the other two eigenvalues are $\lambda_{2a} = \left\{\pm||\nabla F(S(x_0))||, \pm\frac{\delta}{d}||\nabla F(S(x_0))||\right\}$ and for vehicle 2b $\lambda_{2b} = \left\{\pm||\nabla F(S(x_0))||, \mp\frac{\delta}{d}||\nabla F(S(x_0))||\right\}$. The sign of the eigenvalues depends on the heading of the vehicle relative to the gradient as the vehicle can point in the same or the opposite direction of the gradient. On the one hand, the sign of the two eigenvalues for vehicle 2a is the same for a given heading solution of $\nabla S(\mathbf{x})^T \hat{e}_p = 0$ meaning one of the solutions will be an attractor while the other will be a repellor. Specifically, the attractor corresponds to the situation when the vehicle heads the opposite direction of the gradient, and the unstable equilibrium to the vehicle heading the gradient. This means vehicle 2a will move towards the boundary ∂D if it points towards it and will escape if it points in the opposite direction. Eventually vehicle 2a will always reach the boundary of the stimulus and will stay there as stable equilibria exist. This result matches our intuitive understanding of how this vehicle works. On the other hand, vehicle 2b always has eigenvalues with opposite signs and therefore both existing equilibrium points on the state space corresponding to one $\mathbf{x} \in \partial D$ are unstable equilibria. There is no way (but from the stable manifold) the vehicle 2b will reach the boundary ∂D and it will wander around D as there is no other equilibrium point. Braitenberg vehicle 2b can therefore be used to implement wandering behaviour in a bounded workspace.

B. Vehicles 3

The analysis of vehicles 3 shows that equilibrium points can only appear at the maximum of the stimulus since $F(s_1) = 0$. Moreover, if the point is a maximum of the stimulus and the derivative of $F(s)$ is bounded, a set of points on the state space becomes an equilibrium set, as the gradient also vanishes. In this case for any heading, any $\hat{e}_p$, the last equation vanishes $\dot{\theta} = 0$. Unless $F(s)$ is designed to vanish for some stimulus value (s_1 in our case) the behaviour of Braitenberg vehicles 3 will have no equilibrium point and it will move around without stopping, which is not a desirable behaviour for target reaching robots. If, instead of a point, the set of $\mathbf{x}$ such that $S(\mathbf{x}) = s_1$ is a level curve but not a maximum of $S(\mathbf{x})$, preferred equilibrium directions will appear as for vehicles 2 in the previous section.

The linear analysis of the equilibrium point brings no information about the stability if the points where $S(\mathbf{x}) = s_1$ are also maxima of $S(\mathbf{x})$, though intuitively it should be stable for vehicle 3a and unstable for vehicle 3b, but formal tests require again more sophisticated techniques [19]. If the gradient does not vanish when $S(\mathbf{x}) = s_1$ (or $F'(s)$ is not bounded) there are at least two headings of the vehicle where equation (6) also vanishes, and therefore there are equilibrium points of the whole system. The linear stability test can be used again in this case. The result is that vehicle 3a will have at least one angular attractor for the level curve, while vehicle 3b will always move away from it. This theoretically obtained result matches our intuition of how Braitenberg vehicles 3 work, as they model positive and negative animal taxis respectively. Consequently Braitenberg vehicle 3a can in principle be used for target reaching, while vehicle 3b seems appropriate for avoidance tasks.

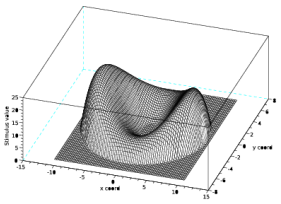

(a) Stimulus function $S(\mathbf{x})$

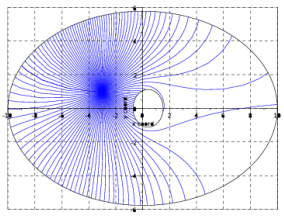

(b) Simulated trajectories

Fig. 3. Simulation of vehicle 2a

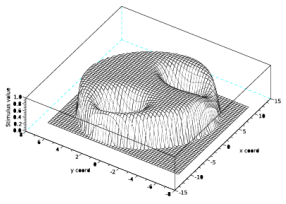

(a) Function composition $F(S(\mathbf{x}))$

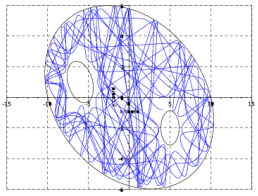

(b) Simulated trajectory

Fig. 4. Simulation of vehicle 2b

IV. Simulations

In order to illustrate the behaviour of the Braitenberg vehicles we performed different simulations by integrating equations (4), (5) and (6) with different stimuli $S(\mathbf{x})$ and functions $F(s)$. Figure 3, for instance, presents the simulations performed for vehicle 2a. The specific stimulus function is the plot on figure 3(a), the non-negative part of the product of two parabolic functions with positive and negative Hessian matrices. The level set $S(\mathbf{x}) = 0$ of the stimulus is formed by the two parabolas with different orientations drawn in figure 3(b). The function $F(s)$ was chosen to be a linear function with positive slope going through the origin ($F(s) = ms$). Figure 3(b) presents the trajectories obtained from simulating vehicle 2a with 60 different headings at position $\mathbf{x}^T = [-3, 1]$. As expected, all the trajectories end at some point where the stimulus takes a zero value, moreover the tangent to the trajectory at these points corresponds to the opposite direction of the gradient as deduced from the formulation.

Figure 4(b) shows the simulated trajectory for Braitenberg vehicle 2b with the function composition $F(S(\mathbf{x}))$ shown in figure 4(a). Instead of selecting a linear $F(s)$ we used the hyperbolic tangent that introduces saturation in the perceived stimulus, as it can also be the case in animal sensors. The level set where the stimulus takes zero value is also shown in figure 4(b) and it is the same as the compound function since $F(0) = 0$. The simulation was stopped at some point since any equilibrium point on the equations describing the behaviour of this vehicle, occurring on the zero level set of the stimulus, is unstable. This can be observed in the trajectory, as when the vehicle approaches the boundary of positive stimulus it turns to come back to points of high stimulus value. Moreover, it has been found through simulations that the vehicle "bounces" against the zero level-set following similar laws as a billiard ball bouncing in a billiard table [17].

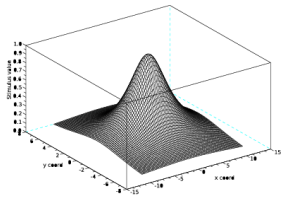

(a) Function composition $F(S(\mathbf{x}))$

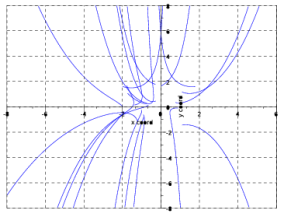

(b) Simulated trajectories

Fig. 5. Simulations of vehicle 3a

Figure 5(b) shows 20 simulated trajectories with random initial conditions withing the 2×2 square around the maximum of the stimulus function in Figure 5(a). Even though the motion of the vehicles goes on, only the parts of the trajectories inside the 8×8 square around the stimulus are plotted. As it can be seen there is a preferred escaping direction almost all the simulated vehicles follow, this is the result of the stimulus not being circularly symmetric but ellipsoidal.

We show in figure 6 ten simulated trajectories starting from random poses of Braitenberg vehicle 3b. The corre-

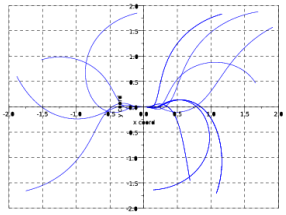

Fig. 6. Simulated trajectories for the vehicle 3b

sponding stimulus functions is the same as for the previous case, figure 5(a), and the connection function $F(s)$ is just a linear function vanishing at the maximum of the stimulus. Since the stimulus has no circular symmetry a preferred direction to reach the maximum and oscillatory behaviour appear in the trajectories as already proven in [20].

V. Discussion and Further Work

This paper presents the first formal joint analysis of Braitenberg vehicles 2 and 3 modelled as systems of non linear differential equations. Besides being used nowadays on an empirical basis for research, Braitenberg vehicles are widely used for teaching purposes. Even though their behaviour can be easily understood in an intuitive basis, applications for robotics mainly rely on educated guesses and empirical parameter adjustment. In this paper we show that the expected behaviour of these vehicles, as intuitively understood, can be explained using the theoretical model and dynamical systems analysis. New conditions to properly implement Braitenberg vehicles have been identified through the analysis of the model, and former applications justified. Specifically, Braitenberg vehicle 2b can be used for wandering, vehicle 3a for goal seeking and 2a for avoidance, by using the appropriate stimuli. This work paves the way for formal robotic applications of Braitenberg vehicles, while supporting and explaining through a mathematical formulation existing empirical works. However, to make sure the presented results apply, the right stimulus must be used, and therefore properties of the stimulus functions have to be tested beforehand. An example of a potential stimulus in mobile robotics can be the distance to some target or to the closest obstacle. However, they are C^1 functions on the workspace. In sum, finding the right stimulus is an important issue for future works.

Real world applications of Braitenberg vehicles are mainly related to navigations tasks on robotics. This paper deals only with the simplest theoretical configuration, a single stimulus but the environments can have different sources of several kinds. This will produce a richer behaviour and very complex equations that probably cannot be understood analytically, but numerical methods can be used for specific stimulus settings. This is part of the evolution of Braitenberg vehicles, specifically vehicle 3c, although no specification is given [1] on how to solve the motor fusion problem. Tasks like obstacle avoidance can be implemented using a combination of vehicles 2a (fear to obstacles, for instance) and 3a (taxis towards a target). According to [1], if restrictions on the function connecting perception and action are relaxed more complex behaviours can appear, these are type 4 vehicles. However, theoretical results already point that even under the simple assumptions presented in this paper, behaviour is very rich and complex. Another interesting extension to this work is to include the effect of noisy sensors on the vehicle that will produce a stochastic Braitenberg vehicle model.

References

[1] V. Braitenberg, *Vehicles. Experiments in synthetic psycology*. The MIT Press, 1984.

[2] M. Resnik, "LEGO, Logo and Life," in *Artificial Life. Proceedings of an Interdisciplinary Workshop on the Synthesis and Simulation of Living Systems*, 1987, pp. 397–406.

[3] M. Travers, "Animal construction kits," in *Artificial Life. Proceedings of an Interdisciplinary Workshop on the Synthesis and Simulation of Living Systems*, 1987, pp. 421–442.

[4] G. Fraenkel and D. Gunn, *The orientation of animals. Kineses, taxes and compass reactions*. Dover publications, 1961.

[5] C. Buiu, "Hybrid educational strategy for a laboratory course on cognitive robotics," *IEEE Transactions on Education*, vol. 51, no. 1, pp. 100–107, 2008.

[6] R. Stolkin, R. Sheryll, and L. Hotaling, "Braitenbergian experiments with simple aquatic robots," 2007.

[7] E. Bicho and G. Schöner, "The dynamic approach to autonomous robotics demonstrated on a low-level vehicle platform," *Robotics and Autonomous Systems*, vol. 21, pp. 23–35, 1997.

[8] I. Rañó and T. Smithers, "Obstacle avoidance through Braitenberg's aggression behavior and motor fusion," in *Proc. of the 2nd European Conf. on Mobile Robots*, 2005, pp. 98–103.

[9] X. Yang, R. V. Patel, and M. Moallem, "A Fuzzy-Braitenberg Navigation Strategy for Differential Drive Mobile Robots," *Journal of Intelligent Robotic Systems*, vol. 47, pp. 101–124, 2006.

[10] L. Capozzo, G. Attolico, and G. Cicirelli, "Building low cost vehicles for simple reactive behaviors," in *Proceedings of the IEEE International Conference on Systems, Man, and Cybernetics*, vol. 6, 1999, pp. 675–680.

[11] A. J. Lilienthal and T. Duckett, "Experimental analysis of gas-sensitive Braitenberg vehicles," *Advanced Robotics*, vol. 18, no. 8, pp. 817–834, 2004.

[12] B. Webb, *A Spiking Neuron Controller for Robot Phonotaxis*. The MIT/AAAI Press, 2001, pp. 3–20.

[13] D. Blustein and J. Ayers, *A conserved network for control of arthropod extereoceptive optical flow reflexes during locomotion*, 2010, vol. 6226, pp. 72–81.

[14] R. French and L. Cañamero, "Introducing neuromodulation to a Braitenberg vehicle," in *Proceedings of the 2005 IEEE International Conference on Robotics and Automation*, 2005, pp. 4188–4193.

[15] I. Rañó, "A steering taxis model and the qualitative analysis of its trajectories," *Adaptive Behavior*, vol. 17, no. 3, pp. 197–211, 2009.

[16] ——, "A bio-inspired controller to generate dense wandering workspace trajectories," in *Proceedings of the 7th Simposium on Intelligent Autonomous vehicles*, 2010.

[17] ——, *An empirical evidence of Braitenberg vehicle 2b behaving as a billiard ball*. Springer, 2010, pp. 293–302.

[18] G. Arechavaleta, J. P. Laumond, H. Hicheur, and A. Berthoz, "An optimality principle governing human walking," *IEEE Transactions on Robotics*, vol. 24, no. 1, pp. 5–14, 2008.

[19] L. Perko, *Differential Equations and Dynamical Systems*. Springer, 2006.

[20] I. Rañó, "On the convergence of braitenberg vehicle 3a immersed in parabolic stimuli," in *Proceedings of the IEEE International Conference on Intelligent Robots and Systems*, 2011.